Gallic acid in theabrownin suppresses cell proliferation and migration in non-small cell lung carcinoma via autophagy inhibition

XUE TIAN[1,2*], JIAAN XU[1,2*], YONGHUA YE[1,2], XIUJUAN XIAO[1,2], LI YAN[3], SHIHUI YU[1,2], JIANYONG CAI[4], QUAN DU[5], XIAOQIAO DONG[5], LI ZHOU[2,3], LETIAN SHAN[2,3] and QIANG YUAN[1]

[1]College of Pharmaceutical Sciences; [2]The First Affiliated Hospital, Zhejiang Chinese Medical University, Hangzhou, Zhejiang 310053; [3]Cell Resource Bank and Integrated Cell Preparation Center of Xiaoshan District, Hangzhou Regional Cell Preparation Center (Shangyu Biotechnology Co., Ltd.), Hangzhou, Zhejiang 311200; [4]Department of Neurosurgery, The Wenzhou Central Hospital, Wenzhou, Zhejiang 325000; [5]Department of Neurosurgery, Affiliated Hangzhou First People's Hospital, Zhejiang University School of Medicine, Hangzhou, Zhejiang 310006, P.R. China

Received August 24, 2022; Accepted March 17, 2023

DOI: 10.3892/ol.2023.13880

Abstract. The bioactive extract of green tea, theabrownin (TB), is known to exhibit pro-apoptotic and antitumor effects on non-small cell lung cancer (NSCLC). Gallic acid (GA) is a crucial component of TB; however, its mechanism of action in NSCLC has been rarely studied. To date, little attention has been paid to the anti-NSCLC activity of GA. Therefore, the present study investigated the effects of GA *in vivo* and *in vitro*. Cell Counting Kit (CCK)-8 assay, DAPI staining and flow cytometry, wound-healing assay and western blotting were used to assess cell viability, apoptosis, migration and protein expression, respectively. In addition, a xenograft model was generated, and TUNEL assay and immunohistochemistry analysis were performed. The CCK-8 data showed that the viability of H1299 cells was significantly inhibited by GA in a dose- and time-dependent manner. DAPI staining, Annexin-V/PI staining and wound-healing data showed that GA exerted pro-apoptotic and anti-migratory effects on H1299 cells in a dose-dependent manner. Furthermore, the results of western blotting showed that GA significantly upregulated the levels of pro-apoptotic proteins [cleaved (c-)PARP, c-caspase8, c-caspase-9 and the ratio of γ-H2A.X/H2A.X]. *In vivo* data confirmed the antitumor effect of GA through apoptosis induction in an autophagy-dependent manner. In conclusion, the present study confirmed the anti-proliferative, pro-apoptotic and anti-migratory effects of GA against NSCLC *in vitro* and *in vivo*, providing considerable evidence for its potential as a novel candidate for the treatment of NSCLC.

Correspondence to: Professor Qiang Yuan, College of Pharmaceutical Sciences, Zhejiang Chinese Medical University, 548 Binwen Road, Binjiang, Hangzhou, Zhejiang 310053, P.R. China
E-mail: yuanqiang0825@sina.com

Professor Letian Shan, The First Affiliated Hospital, Zhejiang Chinese Medical University, 548 Binwen Road, Binjiang, Hangzhou, Zhejiang 310053, P.R. China
E-mail: letian.shan@zcmu.edu.cn

*Contributed equally

Key words: gallic acid, non-small cell lung cancer, H1299, apoptosis

Introduction

Lung cancer is the most common cancer worldwide and is the leading cause of cancer deaths, with low survival and high morbidity rates (1,2). The major forms of lung cancer are non-small cell lung cancer (NSCLC) and small-cell lung cancer (SCLC) (3,4). NSCLC accounts for 85% of all lung cancers, compared with 15% SCLC. A survey showed that nearly 14 million people die from NSCLC every year, and this number will increase in developing countries during the next few decades (5). Aggressive surgery, conventional chemotherapy, and targeted therapeutics are currently the standard treatment options for NSCLC (6-8). However, neoplasm recurrence, insufficient effectiveness, acquired drug resistance, and inevitable side effects have limited the application of those therapies, resulting in unsatisfactory clinical outcomes. Therefore, new drug candidates with high therapeutic efficacy and less adverse effects are urgently needed for patients with NSCLC (9,10).

In recent years, natural products have attracted increasing attention as promising candidates of anti-cancer drugs (11,12). Polyphenolic compounds that exist in natural foods exert beneficial effects on human health by promoting gastrointestinal digestion, preventing excessive thrombosis, lowering blood pressure, and also possess preventive effects against cancers (13-16). Green tea is a commonly consumed beverage containing a large number of bioactive ingredients. Epidemiological studies have discovered that intake of green tea (12 cups per day) can decrease the risk of cancers, and many studies have demonstrated the anti-cancer ability of green tea extract (17). Theabrownin (TB), the bioactive component of green tea, has been reported to possess anti-NSCLC activity

via a p53-dependent mechanism in our previous studies (18,19). The *in vivo* data showed that TB clearly inhibited the growth of NSCLC cell mass in the zebrafish xenograft model with inhibitory rates from 27 to 34%, and its anti-NSCLC efficacy was even better than that of cisplatin (26.1%). Moreover, no toxicity or side effects of TB were observed in its effective dose range (the LD0, 213 μg/ml), while cisplatin induced apoptosis of normal tissues (20). These results suggested that TB was effective and safe for treating NSCLC.

TB contains various active components, such as epigallocatechin gallate (EGCG), epigallocatechin (ECG) and gallic acid (GA) (Fig. S1). After the literature search, EGCG and GA were selected as potential candidates of anti-cancer components (21,22). Following the preliminary screening with CCK-8 (data not shown), we found that GA exerted stronger activity than EGCG. Therefore, this study was conducted to in-depth evaluate the anti-NSCLC effect of GA. NSCLC cell lines (H1299 and A549) were employed to evaluate the effects of GA. This study determined GA's anti-NSCLC properties and validated its efficacy in the p53-mutated NSCLC (H1299) cells, which might facilitate the development of a new anti-NSCLC drug from natural products.

Materials and methods

Materials. Gallic acid (GA, >99% of purity) was obtained from Micklin (Shanghai, China). Roswell Park Memorial Institute (RPMI) 1640 medium was purchased from Hyclone (Logan, USA). Fetal bovine serum (FBS) was purchased from CellMax (Beijing, China). Phosphate buffered saline (PBS) was purchased from Basal Media (Shanghai, China). RIPA lysis buffer and trypsin were purchased from Thermo Fisher Scientific (MA, USA). CCK-8 was obtained from Bimake (TX, USA). DAPI was purchased from Invitrogen (CA, USA). All antibodies were purchased from Cell Signaling Technology Inc (MA, USA).

Cell culture. Human NSCLC H1299 and A549 cell lines were obtained from the Shanghai Cell Bank of the Chinese Academy of Sciences (Shanghai, China). H1299 was cultured in RPMI 1640 medium containing 10% fetal bovine serum and A549 was cultured in Dulbecco's Modified Eagle Medium supplemented with 10% fetal bovine serum, in a 5% CO_2 cell culture incubator. Cells were passaged every 2-3 days and subcultured to 90% confluence.

Cell viability assay. The CCK-8 was used to detect the effect of GA on H1299 cells. Briefly, the cells were seeded in 96-well plates at a density of $6x10^3$ cells/well in 200 μl medium overnight and treated with GA at various concentrations (0, 10, 13, 17, 20, 23, 27, 30 μg/ml) for 24 h. Then, CCK-8 working solution was added to each well and incubated at 37˚C for 2 h. And the optical density (OD) value at 450 nm was measured by microplate reader (Synergy H1, Bio Tek Instruments, Inc). The formula selected: Survival rate (%)=(GA-treated OD/untreated OD) x100%. According to the IC_{50} value of 24 h, three doses were chosen for further use.

DAPI staining. The DAPI staining was performed to determine the apoptosis of H1299 cells induced by GA. The cells were seeded in 24-well plates at a density of $3x10^4$ cells/well in 1 ml medium overnight and treated with GA at low, medium, and high doses for 24 h. After GA treatment, the cells were washed twice in 400 μl PBS and fixed with 4% paraformaldehyde for reaction in 30 min at 37˚C. Then 0.5% Triton X-100 was used to permeabilize the cells in the dark. Cells were mounted with DAPI staining and finally observed staining cells under a fluorescence microscope (Carl Zeiss, Gottingen, Germany). Apoptotic nuclei were visualized and counted on three cover slips for each group.

Flow cytometry. The Annexin-V/PI staining-based flow cytometry was performed to determine the cell apoptosis of H1299 cells induced by GA. The cells were seeded with a density of $5x10^5$ cells/well in 10 ml medium overnight and treated with GA at low, medium, and high doses for 24 h. After GA treatment, the cells were harvested and washed twice with cold PBS, then resuspended with binding buffer. Then the cells were labeled with FITC Annexin-V and PI respectively in the dark. Fluorescence intensity was detected by flow cytometry (BD Biosciences, CA, USA). Apoptosis cell rate (%)=(early apoptotic cells + late apoptotic cells)/total cell number x100%; Living cell rate (%)=normal cells/total cell number x100%.

Wound-healing assay. The wound-healing assay was performed to test the anti-migratory effect of H1299 cells induced by GA. The cells were seeded in 6-well plates at a density of $3x10^5$ cells/well with 3 ml medium, which only contained 1.5% FBS to minimize the proliferation component of cell migration. The cells were treated with low, medium, and high doses of GA, followed by artificial scratch being made in a cross from using a micropipette tip. The cells were observed and imaged at 0, 12, 24, and 48 h under an inverted microscope (Olympus, Tokyo, Japan).

Western blot (WB) analysis. The protein level of the treated GA was explored by WB analysis. Total proteins of H1299 cells were extracted by RIPA buffer with proteinase and phosphatase inhibitor cocktail (Bimake, Houston, USA), and then determined concentration by Bradford protein assay kit. The membrane was blocked with 5% non-fat milk for 2 h and incubated by primary antibodies overnight. And then the membrane was washed and incubated with a secondary antibody for 2 h. Ultimately, the nitrocellulose membrane was visualized by Western Lightning® Plus 8 ECL (PerkinElmer, Inc, Waltham, MA, USA), and detected using a chemiluminescence analyzer (Bio-Rad, Inc, CA. USA). β-actin was employed as a control protein.

Xenografted experiment. Female nude mice aged 6-8 weeks, weighing 18-22 g, were selected for the experiment (Animal production license number: 202204-0284). After one week of adaptive feeding, $5x10^6$ H1299 cells were injected subcutaneously which have highly invasive abilities (23), and the mice were randomly divided into four groups: normal control group treated with normal saline for comparison (NC), GA-low dose group treated with 10 mg/kg GA solution (L), GA-high dose group treated with 40 mg/kg GA solution (H), and cisplatin group treated with 2 mg/kg cisplatin (CIS). After tumor formation, the mice were treated every 4 days by

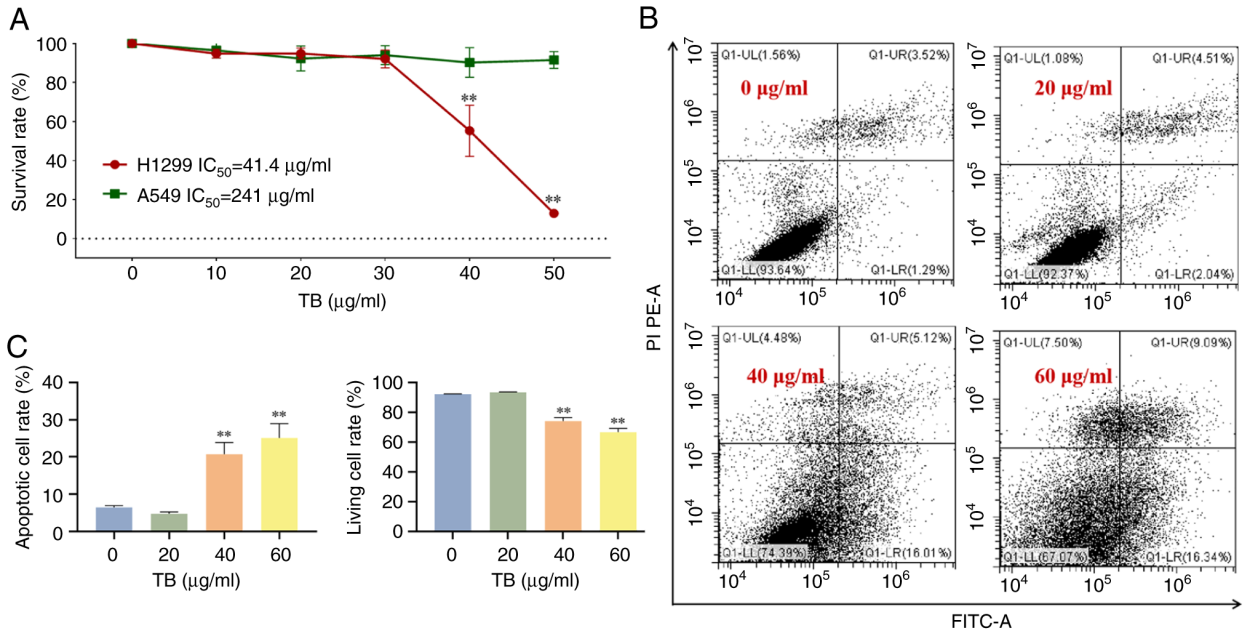

Figure 1. (A) Survival rate of TB (0, 20, 40, 60 μg/ml) on H1299 and A549 cells at 24 h. (B) Flow cytometry analysis on H1299 cells with TB (0, 20, 40, 60 μg/ml) treatment for 24 h. UR quadrant: Early apoptotic cells; LR quadrant: Late apoptotic cells; UL quadrant: Necrosis cells; LL quadrant: Normal cells. (C) Statistical data. Values were presented as the mean ± SD (n=3). **P<0.01 vs. 0 μg/ml. LL, lower-left; LR, lower-right; TB, theabrownin; UL, upper-left; UR, upper-right.

intraperitoneal injection, meanwhile, the tumor size and nude mouse weight were measured. Tumor volumes were calculated as V=1/2 (l) x $(w)^2$, where l and w mean the tumor's longest and shortest diameters, respectively. After the experiment, mice were euthanized (the disappearance of reflex, respiratory arrest and cardiac arrest) by intraperitoneal sodium pentobarbital injection (100 mg/kg) and the tumor tissues were immediately fixed in 4% paraformaldehyde and embedded in paraffin for future experiments. All the experiments on mice were approved by the Medical Norms and Ethics Committee of Zhejiang Chinese Medical University (Approval number: IACUC-20220418-07).

TUNEL assay. The TUNEL staining using in situ cell death detection kit (Roche) was performed to determine the tumor tissue paraffin sections apoptosis. After dewaxing and rehydration, the sections were repaired with sodium citrate buffer (pH=6) for 4 h in 60˚C oven, then permeabilized using TritionX-100 (Biyuntian, China). Add 50 μl TUNEL working solution which consists of TUNEL enzyme solution and TUNEL label mix on the circled tissue and incubated at 4˚C overnight. The next day, after washing with PBS, the nucleus was counterstained with DAPI. Images were acquired using fluorescence microscope (Carl Zeiss, Gottingen, Germany). Apoptotic cell rate=(TUNEL positive nuclei/DAPI positive nuclei) x100%.

Immunohistochemistry analysis. Immunohistochemistry (IHC) was performed using an immunohistochemistry kit (Zhongshan Golden Bridge, China). After conventional dewaxing and rehydration, the sections were repaired with sodium citrate buffer (pH=6) for 4 h in a 60˚C oven, then permeabilized using TritionX-100. A goat serum from the kit was used to block slides before the primary antibody (PCNA: dilution 1:4,000; Cell Signaling; ATG5: dilution 1:100; Immunoway; p-AMPK: dilution 1:100; Cell Signaling) incubation overnight at 4˚C. The next day, the slides were washed with PBS, followed by secondary antibodies incubation for 30 min. After incubation, the slides were washed in PBS, then the freshly prepared diaminobenzidine (DAB) color developing solution was used. The color-development time was checked under the microscope and the slides were washed in ultrapure water to stop the reaction.

Statistical analyses. The mean and standard deviation (SD) of the data was calculated. One-way ANOVA was used for data comparison among multiple groups, followed by Dunnett test. When the P-value was less than 0.05, the difference was judged significant; when the P-value was less than 0.01, the difference was regarded to be of higher importance.

Results and discussion

The inhibitory effect of TB on NSCLC cell lines. Previously, our team has proven that TB has a strong pro-apoptotic effect on NSCLC through p53 signaling pathway (18). At the same time, a high content of GA in TB was detected by UPLC-Q/TOF-MS/MS and its pro-apoptotic effects on NSCLC cells were demonstrated, indicating that GA is a major active ingredient of TB (Fig. S1). While comparing the efficacies of TB on A549 (p53-wild type) and H1299 (p53-null) cells, we found that TB exerted stronger effects on H1299 cells (Fig. 1A). As shown in Fig. 1B and C, flow cytometry analysis revealed that TB at 20, 40, and 60 μg/ml induced obvious apoptosis of H1299 cells in a dose-dependent manner. The observed necrosis might be the secondary necrosis caused by apoptosis, and this study mainly focused on the apoptosis induction other than necrosis occurrence. In addition, another

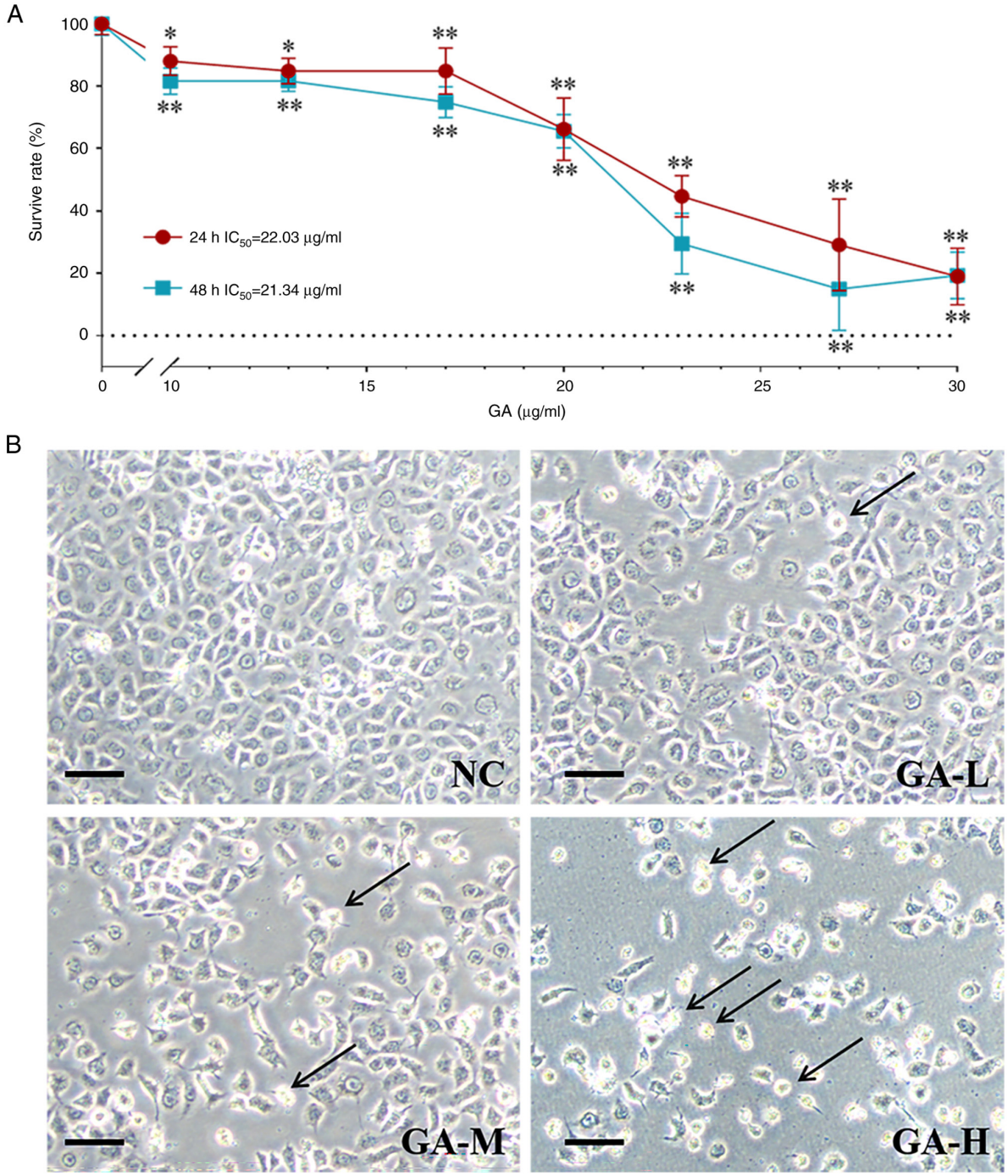

Figure 2. (A) The survival rate of GA (0-30 μg/ml) on H1299 cells at 24 and 48 h. (B) Morphological observation (light microscope) of H1299 cells with GA (0, 10, 13, 20 μg/ml) for 24 h. Scale bar: 50 μm. Values were presented as the mean ± SD (n=3). *P<0.05 and **P<0.01 vs. 0 μg/ml. NC, normal control; GA-L, low dose of gallic acid; GA-M, medium dose of gallic acid; GA-H, high dose of gallic acid.

study has shown that GA could induce both apoptosis and necrosis on tumor cells (24), which was consistent with our results. These results indicated the selective effect of TB on H1299 cells. Whether GA also has better effects on the p53-null NSCLC cells than on the p53-wild type NSCLC cells, remains undetermined. Further studies are needed to explore the selective effects of GA.

The anti-NSCLC effects of GA in vitro

Anti-proliferative effect of GA. To evaluate the anti-proliferative effect of GA on H1299 cells, CCK-8 assay and morphological observation were performed. As shown in Fig. 2A, GA significantly inhibited the viability of H1299 cells at a dose range from 10 to 30 μg/ml. The IC_{50} values were 22.03 and 21.34 μg/ml for 24 and 48 h, respectively. Accordingly, 10, 13, and 20 μg/ml were selected as low, medium, and high doses for subsequent experiments. Through light microscopic, an increased number of abnormal H1299 cells were observed to be irregular and had shrunk (Fig. 2B).

Pro-apoptotic effect of GA. To observe the apoptosis of H1299 cells induced by GA, DAPI staining and flow cytometry were performed. As shown in Fig. 3A and B, GA significantly

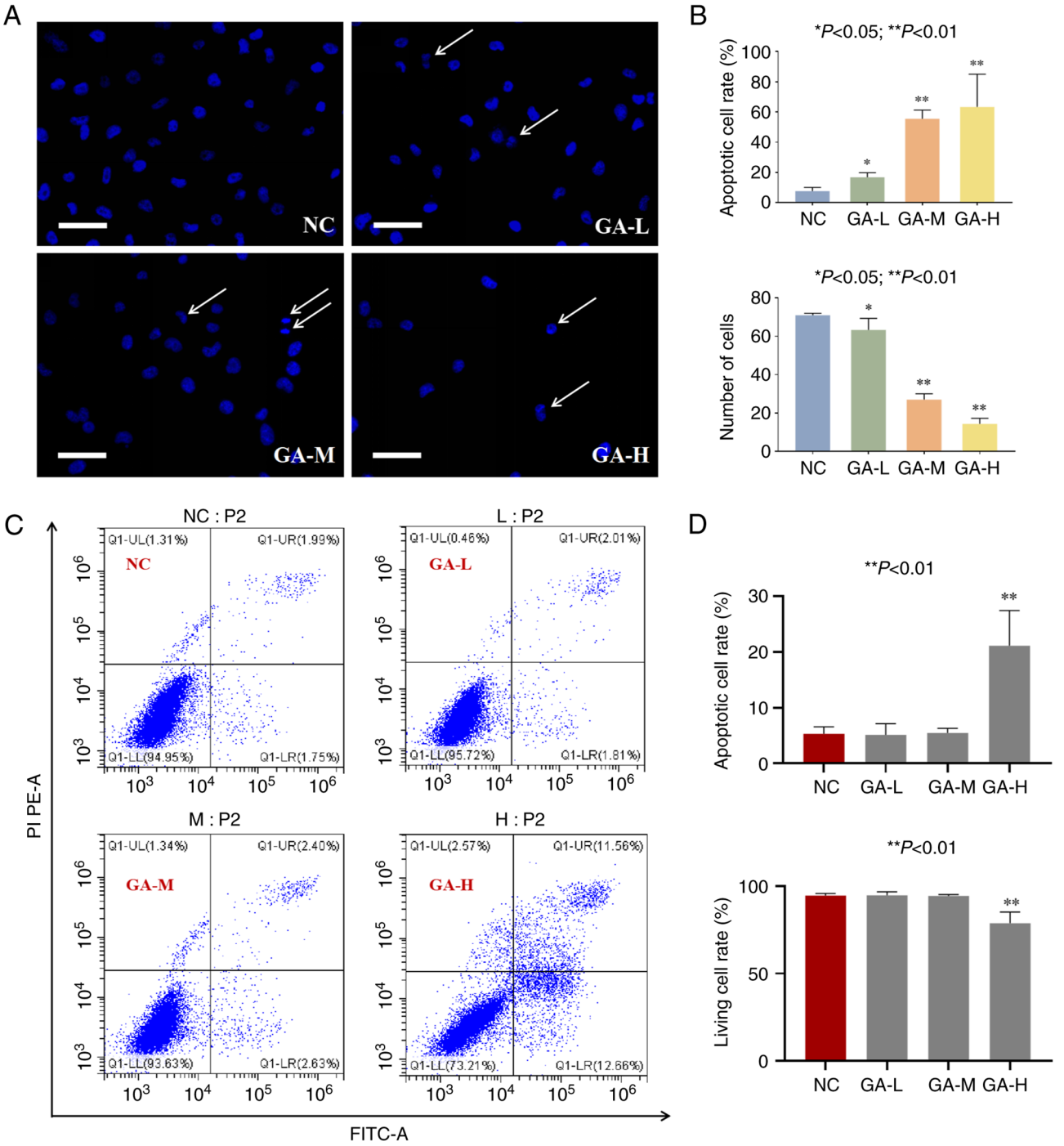

Figure 3. (A) DAPI staining observation of H1299 cells after 24 h treatment of GA. (B) Statistical data. (C) Flow cytometry assays of the apoptosis rate in H1299 cells after 24 h treatment of GA with Annexin-V/PI staining. UR quadrant: Early apoptotic cells; LR quadrant: Late apoptotic cells; UL quadrant: Necrosis cells; LL quadrant: Normal cells. (D) Statistical data. Scale bar: 50 μm. Values were presented as the mean ± SD (n=5). *P<0.05 and **P<0.01 vs. NC. NC, normal control; GA-L, low dose of gallic acid; GA-M, medium dose of gallic acid; GA-H, high dose of gallic acid; LL, lower-left; LR, lower-right; TB, theabrownin; UL, upper-left; UR, upper-right.

increased the number of apoptotic cells as seen by nuclear shrinkage (indicated by arrows) and decreased the number of normal cells (each P<0.05 or 0.01 vs. NC).

We conducted the Annexin-V assay at the same time point (24 h) with the DAPI test. It is because that the Annexin-V result at an earlier time (6 h) could not show significant difference between the groups (data not shown), suggesting that 24 h was a better time point to determine the pro-apoptotic effect of GA. Another reason to select 24 h was that the other assays were conducted at 24 h, so that we could obtain the results at a consistent time point (20). As shown in Fig. 3C and D, early apoptosis, late apoptosis, and necrosis rates were increased following the treatment with GA, suggesting that GA exerted a pro-apoptotic effect on H1299 cells in a dose-dependent manner.

Anti-migratory effect of GA. To observe the anti-migratory effect of GA, wound healing assay was performed. As shown in Fig. 4A, GA significantly inhibited the wounding area ratio of H1299 cells following treatment for 12, 24, and 48 h at

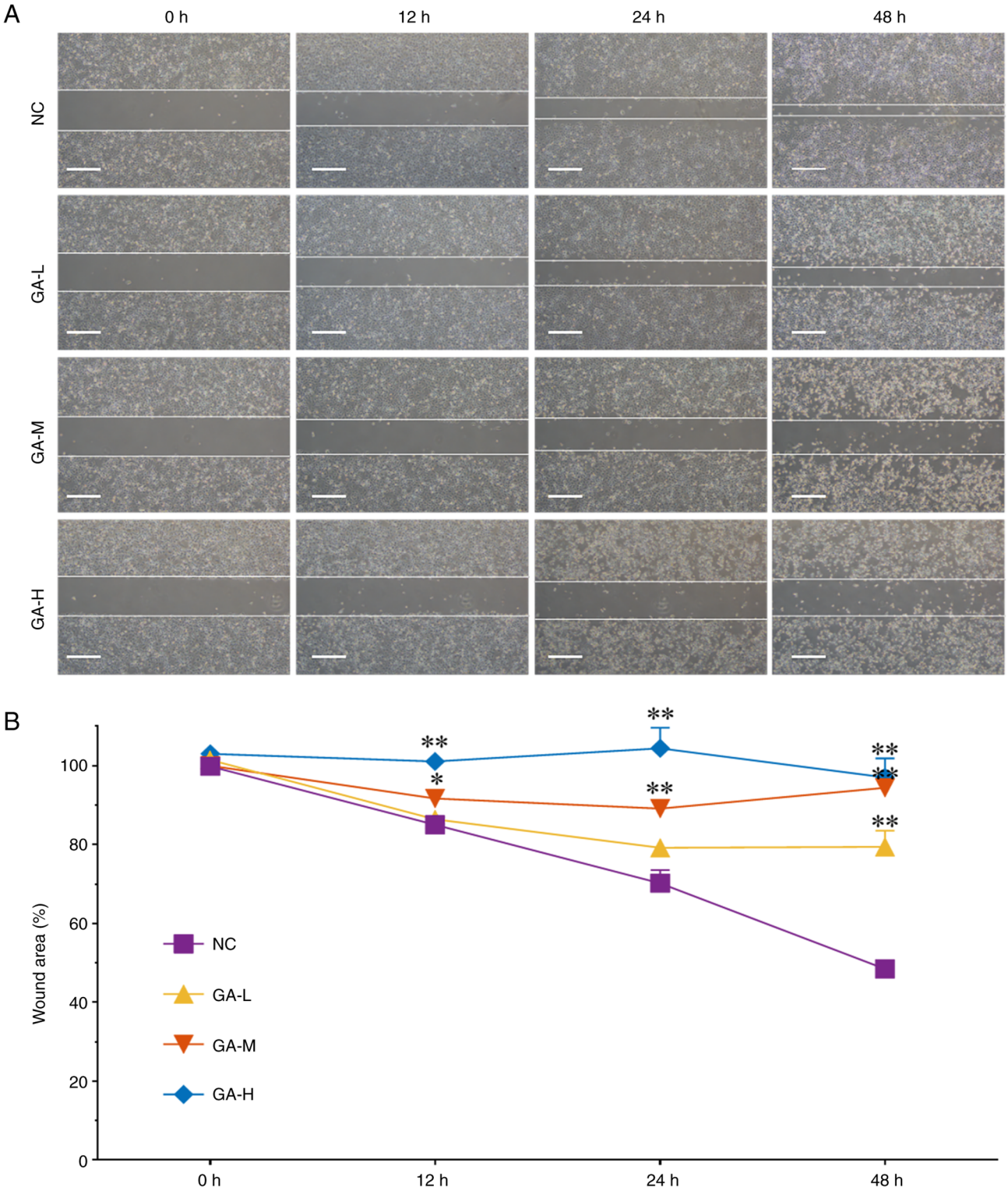

Figure 4. (A) Wound healing observation of H1299 cells in the control group and GA treatment group at 0, 12, 24, and 48 h. (B) Statistical data. Scale bar: 200 μm. Values were presented as the mean ± SD (n=3). *P<0.05 and **P<0.01 vs. NC. NC, normal control; GA-L, low dose of gallic acid; GA-M, medium dose of gallic acid; GA-H, high dose of gallic acid.

low, medium, and high doses (each P<0.05 or 0.01 vs. NC), suggesting that GA inhibited H1299 cells migration in dose- and time-dependent manners.

Molecular actions of GA. It is now widely believed that apoptosis is a hindrance in cancer proliferation since it halts the physiological process, preventing progression to further steps such as embryogenesis, morphogenesis, and tissue homeostasis (25-27). The primary physiological function of apoptosis is to eliminate damaged cells early in development or to maintain somatic homeostasis later.

In this study, the results of cell experiments showed that GA induced apoptosis of H1299 cells by increasing the ratio

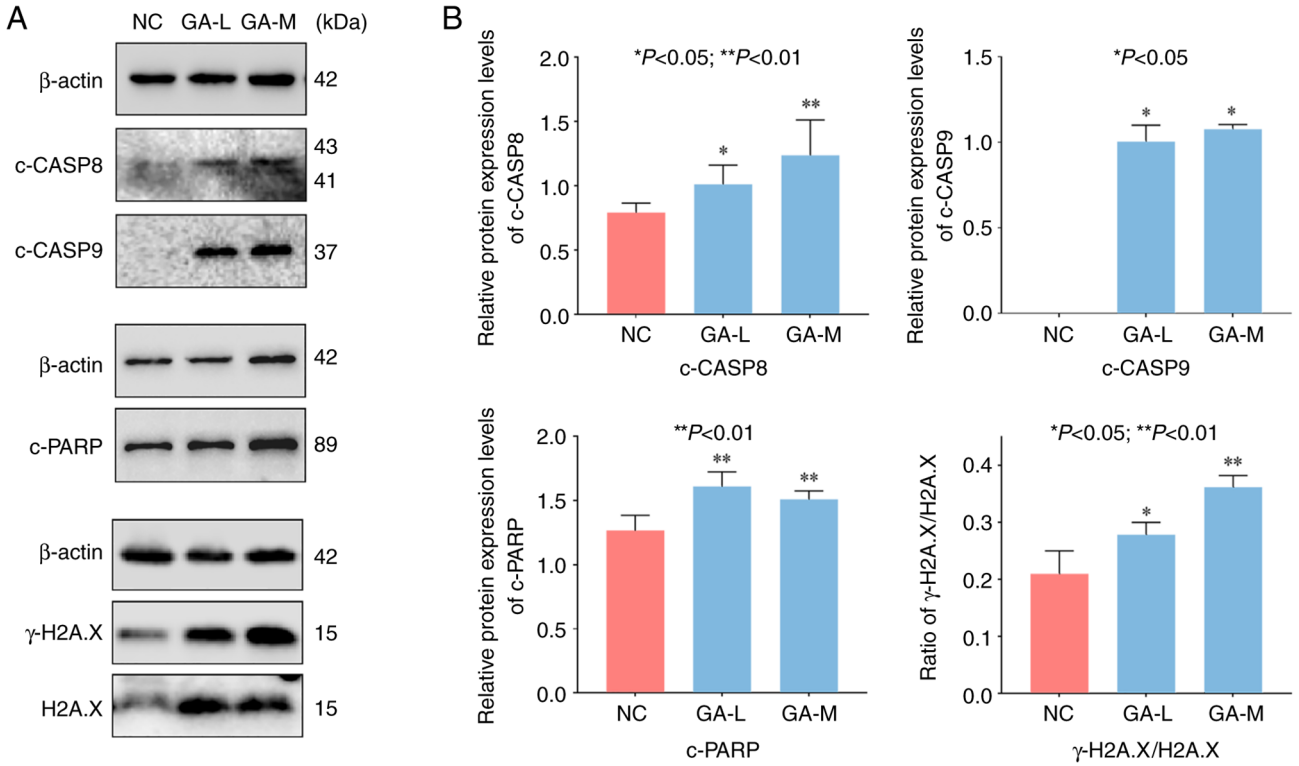

Figure 5. (A) The expression of GA-targeted proteins in H1299 cells after 24 h treatment of GA. (B) Statistical data. Values were presented as the mean ± SD (n=3). *P<0.05 and **P<0.01 vs. NC. NC, normal control; GA-L, low dose of gallic acid; GA-M, medium dose of gallic acid; GA-H, high dose of gallic acid.

of γ-H2A.X/H2A.X, and cleaved (c-)PARP, c-caspase-8 and c-caspase-9 levels (Fig. 5). The ratio of γ-H2A.X/H2A.X is a strong indicator of apoptosis-induced DNA fragmentation, participating in the earliest cellular responses to DNA damage (28). PARP is responsible for DNA repair and maintaining cell viability during external stress. It can be cleaved into two fragments (89 and 25 kDa), which serves as a marker of apoptosis (29). The WB data showed that the ratio of γ-H2A.X/H2A.X and c-PARP protein levels were significantly up-regulated, indicating that GA triggered DNA damage to induce apoptosis of H1299 cells. Meanwhile, in caspase-mediated apoptosis, caspase-8 and caspase-9 are the molecules responsible for initiating apoptosis (30,31). Caspase-8 is the main executor of apoptosis, which releases cytochrome c through the intracellular pathway to trigger apoptosis (32,33), while caspase-9, as an essential promoter in the apoptosis signaling pathway, participates in compound-activated apoptosis (34). The activation of these molecules revealed that GA induced H1299 cells apoptosis in a dose-dependent manner. In addition, no cell survived in the high-dose group due to the highly inhibitory effect of GA, and thereby the protein level was too low to be detected. Therefore, the result of the high-dose group was not shown. In sum, these data indicated that GA exerted significant anti-proliferative, pro-apoptotic, and anti-migratory effects on H1299 cells *in vitro*.

The anti-tumor effects of GA in vivo. The nude mouse xenograft model was established to assess the anti-tumor potential of GA *in vivo*. As shown in Fig. 6, GA significantly reduced the tumor size of nude mice in a dose-dependent manner. Meanwhile, the high dose group of GA had tumors of approximately the same size as those in the cisplatin control group, but the mice of the cisplatin group lost much more weight.

The apoptotic cells in tumor were assessed using TUNEL assay. As shown in Fig. 7A and B, cisplatin was included as positive control, and the number of apoptotic cells (green fluorescence) increased after GA treatment, demonstrating that GA induced apoptosis in H1299 cells. Meanwhile, PCNA expression was verified to determine cell proliferation rate *in vivo* through IHC analysis (Fig. 7C and D), and the data showed that GA reduced the expression of PCNA.

In addition, accumulated research has shown that apoptosis can be activated through autophagy inhibition (35). Therefore, we conjectured that GA's pro-apoptotic effect was associated with autophagy. Autophagy is a mechanism that controls cellular homeostasis through the autolysis of lysosomal enzymes, which is considered as a tumor survival mechanism that helps tumor cells resist drugs (36). However, accumulating evidence suggests that autophagy can also promote tumor cell apoptosis by degrading the reticulum, Golgi apparatus, and other organelles, causing precancerous cells to have a negative protein balance and thereby suppressing uncontrolled proliferation (37,38). Autophagy related 5 (ATG5) is a key initiator of autophagy required for autophagosome formation and has an important effect on the occurrence and changes in autophagy phases (39,40). Adenosine monophosphate (AMP) activated protein kinase (AMPK) is a trigger of autophagy and phosphorylation of AMPK has in fact been shown to promote autophagy induction (41-43). In the present study, the level of ATG5 and p-AMPK were all reduced by GA (Fig. 7C and D), indicating the pro-apoptotic efficacy of GA was mediated through autophagy inhibition.

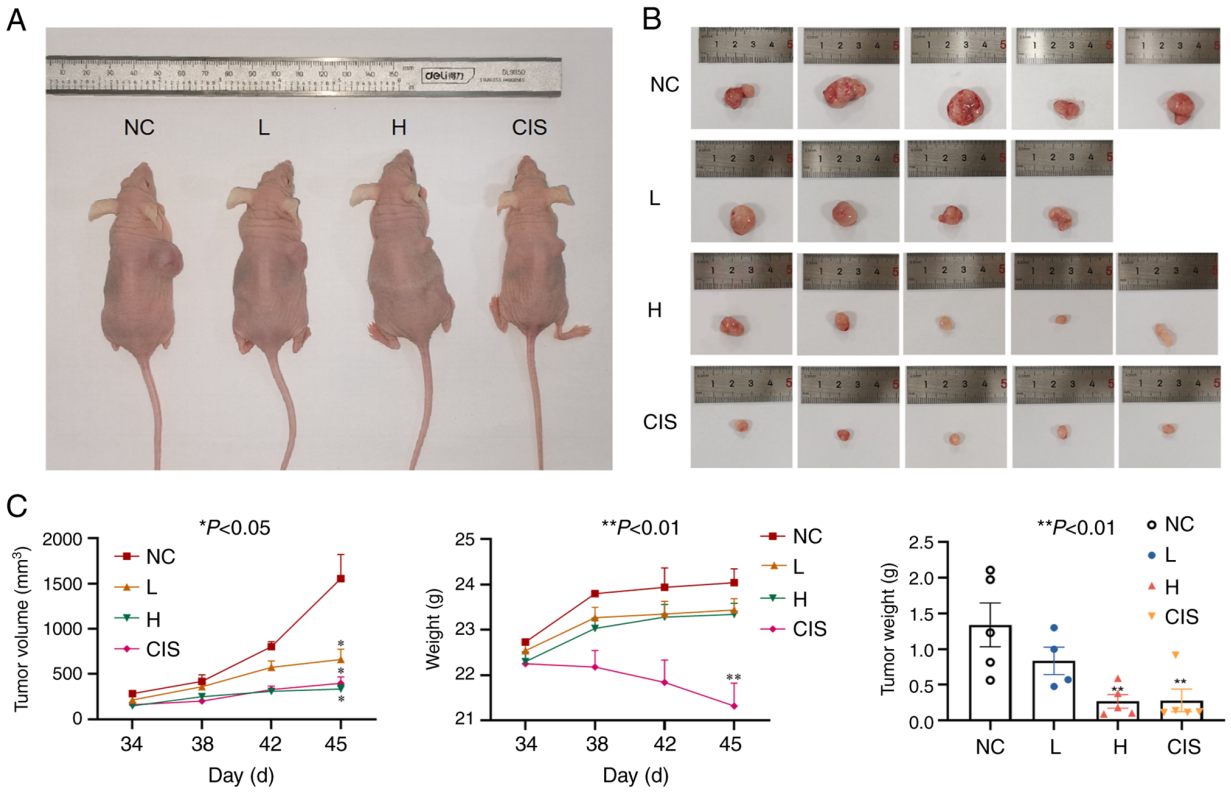

Figure 6. (A) The representative picture of the nude mice of different treatment groups. (B) The photograph of solid tumors. (C) The tumor volume growth curve inhibition map, mice body weight change map, and the tumor weights. Values were presented as the mean ± SD (n=5). *P<0.05 and **P<0.01 vs. NC. NC, normal control; L, low dose of gallic acid; H, high dose of gallic acid; CIS, cisplatin group (positive control).

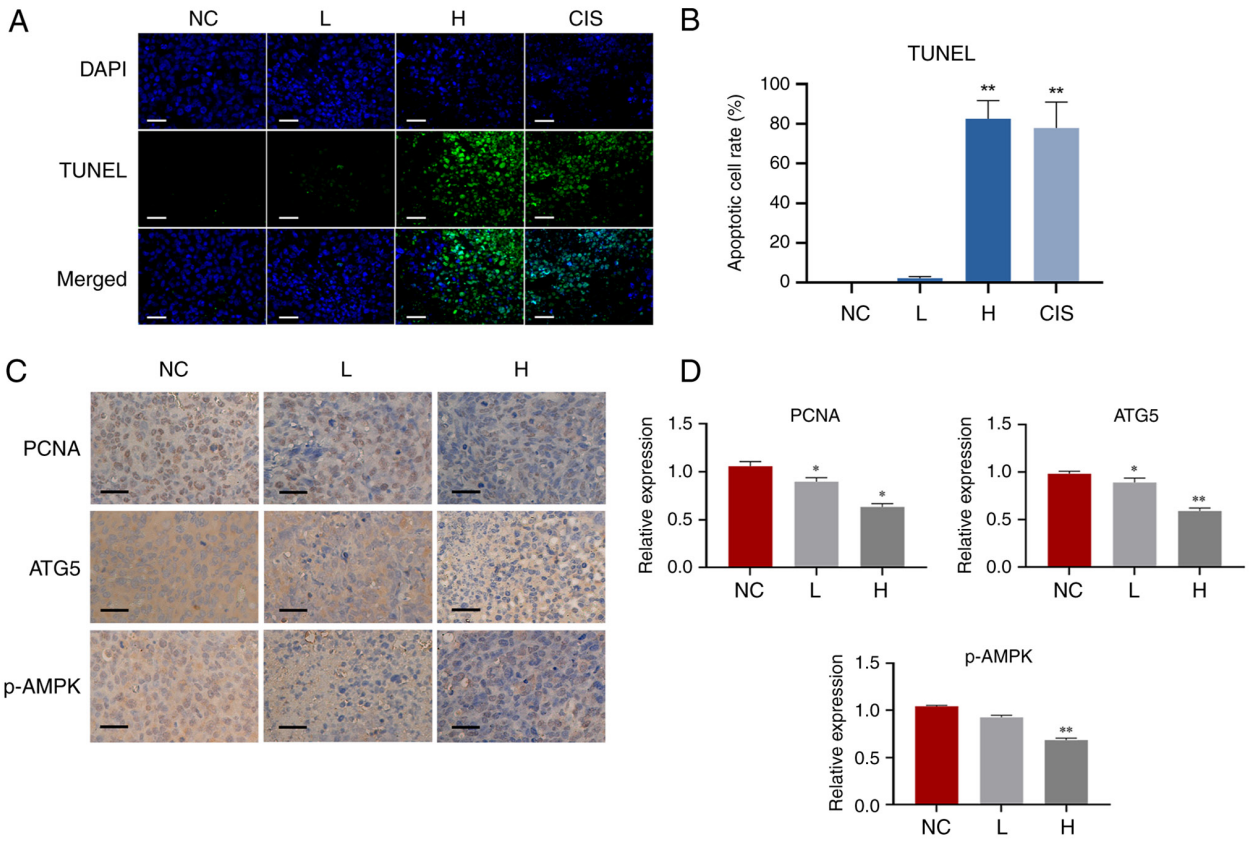

Figure 7. (A) Apoptotic cells determined by TUNEL assay (DAPI staining for nuclei: blue fluorescence; TUNEL staining for apoptotic cells: green fluorescence), and (B) quantitative analysis of TUNEL staining. (C) The immunohistochemistry assay and (D) quantitative analysis of immunohistochemistry results. Scale bar: 50 μm. Values were presented as the mean ± SD (n=5). *P<0.05 and **P<0.01 vs. NC. NC, normal control; L, low dose of gallic acid; H, high dose of gallic acid; CIS, cisplatin group (positive control).

For decades, polyphenols have been used as natural products to protect plants from oxidative stress and UV damage, and to attract pollen and animal material for seed dispersal. The anti-oxidant, anti-inflammatory and anti-cancer effects of polyphenols are receiving increasing attention in recent years (44,45). Previous studies reported that the combination of ascorbic acid, lysine, proline and at least one phenolic compound can be used as an agent for cancer prevention and treatment. As the most common derivatives of the hydroxybenzoic acid, GA received increasing attention in this regard. Numerous *in vitro* and *in vivo* studies have shown that GA has broad pharmacological and therapeutic effects on a variety of cancer cells through a pleiotropic molecular mechanism (e.g., cell apoptotic processes, cell cycle, angiogenesis and invasion) (46,47). In this study, the anti-NSCLC effects of GA was evaluated.

Our previous research mainly focused on the p53-dependent mechanism of TB, and the IC_{50} value of TB against A549 cells was 239.9 μg/ml at 24 h (48). Consistently, the IC_{50} value of TB against A549 cells was 241 μg/ml at 24 h in the present study, which was higher than the IC_{50} value of TB against H1299 cells (41.4 μg/ml), indicating that the anti-proliferation effect of TB on H1299 cells was better than that of A549. Since H1299 is a p53-null cell line and A549 is a p53-wild type cell line, we hypothesize that the inhibition difference of TB on both cells may be related to the P53 pathway. Meanwhile, this study demonstrates for the first time that GA can induce apoptosis in NSCLC cells by inhibiting autophagy. It provides new insights into the anti-NSCLC efficacy of GA and lays the foundation for our next mechanism study, contributing to the application prospects of GA as a therapeutic agent for NSCLC.

Acknowledgements

Not applicable.

Funding

This work was supported by National Natural Science Foundation of China (grant no. 81893049), Zhejiang traditional Chinese medicine science and technology plan project (grant no. 2015ZA194), and Science and Technology Development Project of Hangzhou (grant no. 2020ZDSJ0900).

Availability of data and materials

The datasets used and/or analyzed during the current study are available from the corresponding author on reasonable request.

Authors' contributions

XT, JX and LS conceptualized the study. XT and JX analyzed data. JC, XD, QD, LZ, QY and LS provided financial support. LZ and QY designed the method and JC, XD, and QD participated in the method design. YY, XX, LY and SY designed and performed experiments that generated the preliminary data. LZ, QY and LS supervised the study. XT and JX wrote the original draft. XT and JX confirm the authenticity of all the raw data. All authors read and approved the final manuscript.

Ethics approval and consent to participate

All experiments on the mice were approved by the Medical Norms and Ethics Committee of Zhejiang Chinese Medical University (approval number: IACUC-20220418-07).

Patient consent for publication

Not applicable.

Competing interests

The authors declare that they have no competing interests.

References

1. Hua Q, Jin M, Mi B, Xu F, Li T, Zhao L, Liu J and Huang G: LINC01123, a c-Myc-activated long non-coding RNA, promotes proliferation and aerobic glycolysis of non-small cell lung cancer through miR-199a-5p/c-Myc axis. J Hematol Oncol 12: 91, 2019.
2. Ruiz EJ, Diefenbacher ME, Nelson JK, Sancho R, Pucci F, Chakraborty A, Moreno P, Annibaldi A, Liccardi G, Encheva V, *et al*: LUBAC determines chemotherapy resistance in squamous cell lung cancer. J Exp Med 216: 450-465, 2019.
3. Chen J, Liu A, Wang Z, Wang B, Chai X, Lu W, Cao T, Li R, Wu M, Lu Z, *et al*: LINC00173.v1 promotes angiogenesis and progression of lung squamous cell carcinoma by sponging miR-511-5p to regulate VEGFA expression. Mol Cancer 19: 98, 2020.
4. Deng W, Xu T, Xu Y, Wang Y, Liu X, Zhao Y, Yang P and Liao Z: Survival patterns for patients with resected n2 non-small cell lung cancer and postoperative radiotherapy: A prognostic scoring model and heat map approach. J Thorac Oncol 13: 1968-1974, 2018.
5. Lee SM, Khan I, Upadhyay S, Lewanski C, Falk S, Skailes G, Marshall E, Woll PJ, Hatton M, Lal R, *et al*: First-line erlotinib in patients with advanced non-small-cell lung cancer unsuitable for chemotherapy (TOPICAL): A double-blind, placebo-controlled, phase 3 trial. Lancet Oncol 13: 1161-1170, 2012.
6. Cho J, Min HY, Lee HJ, Hyun SY, Sim JY, Noh M, Hwang SJ, Park SH, Boo HJ, Lee HJ, *et al*: RGS2-mediated translational control mediates cancer cell dormancy and tumor relapse. J Clin Invest 131: e136779, 2021.
7. Karnthaler-Benbakka C, Groza D, Kryeziu K, Pichler V, Roller A, Berger W, Heffeter P and Kowol CR: Tumor-targeting of EGFR inhibitors by hypoxia-mediated activation. Angew Chem Int Ed Engl 53: 12930-12935, 2014.
8. Phuchareon J, McCormick F, Eisele DW and Tetsu O: EGFR inhibition evokes innate drug resistance in lung cancer cells by preventing Akt activity and thus inactivating Ets-1 function. Proc Natl Acad Sci USA 112: E3855-E3863, 2015.
9. Jeong Y, Hellyer JA, Stehr H, Hoang NT, Niu X, Das M, Padda SK, Ramchandran K, Neal JW, Wakelee H and Diehn M: Role of KEAP1/NFE2L2 mutations in the chemotherapeutic response of patients with non-small cell lung cancer. Clin Cancer Res 26: 274-281, 2020.
10. Nokihara H, Lu S, Mok TSK, Nakagawa K, Yamamoto N, Shi YK, Zhang L, Soo RA, Yang JC, Sugawara S, *et al*: Randomized controlled trial of S-1 versus docetaxel in patients with non-small-cell lung cancer previously treated with platinum-based chemotherapy (East Asia S-1 Trial in Lung Cancer). Ann Oncol 28: 2698-2706, 2017.
11. Zhang W, Gao Y, Li P, Shi Z, Guo T, Li F, Han X, Feng Y, Zheng C, Wang Z, *et al*: VGLL4 functions as a new tumor suppressor in lung cancer by negatively regulating the YAP-TEAD transcriptional complex. Cell Res 24: 331-343, 2014.
12. Engelen M, Safar AM, Bartter T, Koeman F and Deutz NEP: High anabolic potential of essential amino acid mixtures in advanced nonsmall cell lung cancer. Ann Oncol 26: 1960-1966, 2015.
13. Gu HF, Mao XY and Du M: Prevention of breast cancer by dietary polyphenols-role of cancer stem cells. Crit Rev Food Sci Nutr 60: 810-825, 2020.
14. Gunther S, Ruhe C, Derikito MG, Bose G, Sauer H and Wartenberg M: Polyphenols prevent cell shedding from mouse mammary cancer spheroids and inhibit cancer cell invasion in confrontation cultures derived from embryonic stem cells. Cancer Lett 250: 25-35, 2007.

15. Thangapazham RL, Singh AK, Sharma A, Warren J, Gaddipati JP and Maheshwari RK: Green tea polyphenols and its constituent epigallocatechin gallate inhibits proliferation of human breast cancer cells in vitro and in vivo. Cancer Lett 245: 232-241, 2007.
16. Adhami VM, Malik A, Zaman N, Sarfaraz S, Siddiqui IA, Syed DN, Afaq F, Pasha FS, Saleem M and Mukhtar H: Combined inhibitory effects of green tea polyphenols and selective cyclooxygenase-2 inhibitors on the growth of human prostate cancer cells both in vitro and in vivo. Clin Cancer Res 13: 1611-1619, 2007.
17. Shanafelt TD, Call TG, Zent CS, LaPlant B, Bowen DA, Roos M, Secreto CR, Ghosh AK, Kabat BF, Lee MJ, *et al*: Phase I trial of daily oral Polyphenon E in patients with asymptomatic Rai stage 0 to II chronic lymphocytic leukemia. J Clin Oncol 27: 3808-3814, 2009.
18. Wu F, Zhou L, Jin W, Yang W, Wang Y, Yan B, Du W, Zhang Q, Zhang L, Guo Y, *et al*: Anti-proliferative and apoptosis-inducing effect of theabrownin against non-small cell lung adenocarcinoma A549 cells. Front Pharmacol 7: 465, 2016.
19. Xu J, Xiao X, Yan B, Yuan Q, Dong X, Du Q, Zhang J, Shan L, Ding Z, Zhou L and Efferth T: Green tea-derived theabrownin induces cellular senescence and apoptosis of hepatocellular carcinoma through p53 signaling activation and bypassed JNK signaling suppression. Cancer Cell Int 22: 39, 2022.
20. Xiao X, Guo L, Dai W, Yan B, Zhang J, Yuan Q, Zhou L, Shan L and Efferth T: Green tea-derived theabrownin suppresses human non-small cell lung carcinoma in xenograft model through activation of not only p53 signaling but also MAPK/JNK signaling pathway. J Ethnopharmacol 291: 115167, 2022.
21. Almatroodi SA, Almatroudi A, Khan AA, Alhumaydhi FA, Alsahli MA and Rahmani AH: Potential therapeutic targets of epigallocatechin gallate (EGCG), the most abundant catechin in green tea, and its role in the therapy of various types of cancer. Molecules 25: 3146, 2020.
22. Jiang Y, Pei J, Zheng Y, Miao YJ, Duan BZ and Huang LF: Gallic acid: A potential anti-cancer agent. Chin J Integr Med 28: 661-671, 2022.
23. Rios-Doria J, Stevens C, Maddage C, Lasky K and Koblish HK: Characterization of human cancer xenografts in humanized mice. J Immunother Cancer 8: e000416, 2020.
24. Hsieh SC, Wu CC, Hsu SL and Yen JH: Molecular mechanisms of gallic acid-induced growth inhibition, apoptosis, and necrosis in hypertrophic scar fibroblasts. Life Sci 179: 130-138, 2017.
25. Sun G, Ding XA, Argaw Y, Guo X and Montell DJ: Akt1 and dCIZ1 promote cell survival from apoptotic caspase activation during regeneration and oncogenic overgrowth. Nat Commun 11: 5726, 2020.
26. Marquez-Jurado S, Diaz-Colunga J, das Neves RP, Martinez-Lorente A, Almazán F, Guantes R and Iborra FJ: Mitochondrial levels determine variability in cell death by modulating apoptotic gene expression. Nat Commun 9: 389, 2018.
27. Liu X, He Y, Li F, Huang Q, Kato TA, Hall RP and Li CY: Caspase-3 promotes genetic instability and carcinogenesis. Mol Cell 58: 284-296, 2015.
28. Peron S, Pan-Hammarstrom Q, Imai K, Du L, Taubenheim N, Sanal O, Marodi L, Bergelin-Besançon A, Benkerrou M, de Villartay JP, *et al*: A primary immunodeficiency characterized by defective immunoglobulin class switch recombination and impaired DNA repair. J Exp Med 204: 1207-1216, 2007.
29. Nick AM, Stone RL, Armaiz-Pena G, Ozpolat B, Tekedereli I, Graybill WS, Landen CN, Villares G, Vivas-Mejia P, Bottsford-Miller J, *et al*: Silencing of p130cas in ovarian carcinoma: A novel mechanism for tumor cell death. J Natl Cancer Inst 103: 1596-1612, 2011.
30. Chaudhuri AR and Nussenzweig A: The multifaceted roles of PARP1 in DNA repair and chromatin remodelling. Nat Rev Mol Cell Biol 18: 610-621, 2017.
31. Wei H and Yu X: Functions of PARylation in DNA damage repair pathways. Genomics Proteomics Bioinformatics 14: 131-139, 2016.
32. Salvesen GS: Caspase 8: Igniting the death machine. Structure 7: R225-R229, 1999.
33. Fritsch M, Gunther SD, Schwarzer R, Albert MC, Schorn F, Werthenbach JP, Schiffmann LM, Stair N, Stocks H, Seeger JM, *et al*: Caspase-8 is the molecular switch for apoptosis, necroptosis and pyroptosis. Nature 575: 683-687, 2019.
34. Mita AC, Mita MM, Nawrocki ST and Giles FJ: Survivin: Key regulator of mitosis and apoptosis and novel target for cancer therapeutics. Clin Cancer Res 14: 5000-5005, 2008.
35. Peng J, Zhu S, Hu L, Ye P, Wang Y, Tian Q, Mei M, Chen H and Guo X: Wild-type rabies virus induces autophagy in human and mouse neuroblastoma cell lines. Autophagy 12: 1704-1720, 2016.
36. Kim KH and Lee MS: Autophagy-a key player in cellular and body metabolism. Nat Rev Endocrinol 10: 322-337, 2014.
37. Hippert MM, O'Toole PS and Thorburn A: Autophagy in cancer: Good, bad, or both? Cancer Res 66: 9349-9351, 2006.
38. Hait WN, Jin S and Yang JM: A matter of life or death (or both): Understanding autophagy in cancer. Clin Cancer Res 12: 1961-1965, 2006.
39. Hu Z, Zhang J and Zhang Q: Expression pattern and functions of autophagy-related gene atg5 in zebrafish organogenesis. Autophagy 7: 1514-1527, 2011.
40. Liu H, Liu S, Qiu X, Yang X, Bao L, Pu F, Liu X, Li C, Xuan K, Zhou J, *et al*: Donor MSCs release apoptotic bodies to improve myocardial infarction via autophagy regulation in recipient cells. Autophagy 16: 2140-2155, 2020.
41. Kumar D, Shankar S and Srivastava RK: Rottlerin-induced autophagy leads to the apoptosis in breast cancer stem cells: Molecular mechanisms. Mol Cancer 12: 171, 2013.
42. Awan FM, Obaid A, Ikram A and Janjua HA: Mutation-structure-function relationship based integrated strategy reveals the potential impact of deleterious missense mutations in autophagy related proteins on hepatocellular carcinoma (HCC): A comprehensive informatics approach. Int J Mol Sci 18: 139, 2017.
43. Kim J, Kundu M, Viollet B and Guan KL: AMPK and mTOR regulate autophagy through direct phosphorylation of Ulk1. Nat Cell Biol 13: 132-141, 2011.
44. Xu L, Yue Q, Bian F, Sun H, Zhai H and Yao Y: Melatonin enhances phenolics accumulation partially via ethylene signaling and resulted in high antioxidant capacity in grape berries. Front Plant Sci 8: 1426, 2017.
45. Speranza S, Knechtl R, Witlaczil R and Schonlechner R: Reversed-phase HPLC characterization and quantification and antioxidant capacity of the phenolic acids and flavonoids extracted from eight varieties of sorghum grown in Austria. Front Plant Sci 12: 769151, 2021.
46. Jang YG, Ko EB and Choi KC: Gallic acid, a phenolic acid, hinders the progression of prostate cancer by inhibition of histone deacetylase 1 and 2 expression. J Nutr Biochem 84: 108444, 2020.
47. Bernhaus A, Fritzer-Szekeres M, Grusch M, Saiko P, Krupitza G, Venkateswarlu S, Trimurtulu G, Jaeger W and Szekeres T: Digalloylresveratrol, a new phenolic acid derivative induces apoptosis and cell cycle arrest in human HT-29 colon cancer cells. Cancer Lett 274: 299-304, 2009.
48. Zhou L, Wu F, Jin W, Yan B, Chen X, He Y, Yang W, Du W, Zhang Q, Guo Y, *et al*: Theabrownin inhibits cell cycle progression and tumor growth of lung carcinoma through c-myc-related mechanism. Front Pharmacol 8: 75, 2017.

Copyright © 2023 Tian et al. This work is licensed under a Creative Commons Attribution-NonCommercial-NoDerivatives 4.0 International (CC BY-NC-ND 4.0) License.